

Chemical Sensing with Surface Acoustic Wave Devices

by

James T. Sun

*Submitted in partial fulfillment of
the requirements for the degree of
Master of Science*

Division of Chemistry and Chemical Engineering
California Institute of Technology

10 September 1993

*To my family and friends, whose faith
and support have withstood weathering times*

*La foi consiste à croire ce que la raison ne croit pas...
Il ne suffit pas qu'une chose soit possible pour la croire.*

Voltaire

Table of Contents

Abstract	1
Introduction	2
Theory of SAW Device Operation	6
Issues in Selective Coatings	8
Experimental Objective	11
Experimental	12
<i>Materials</i>	12
<i>Synthesis</i>	13
<i>Characterizations</i>	15
<i>Coating Preparations</i>	15
<i>Vapor Flow System</i>	16
Results and Discussion	20
<i>Surface Film Deposition</i>	20
<i>Device Design</i>	21
<i>SAW Sensor Performance with Organic Coatings.</i>	22
<i>SAW Sensor Performance with Inorganic Coatings</i>	30
Future Work	38
Conclusions	41
References	43

Abstract

There is much current interest in developing new techniques for the continuous monitoring of chemical environments. However, as there are many applications where the excessive size and power demands of conventional sensors have precluded their use, interest in microsensors such as the surface acoustic wave (SAW) device has been spurred by their small size, ruggedness, sensitivity, and low power consumption. In this work, 158 MHz SAW oscillators coated with organic polymers and inorganic crystallites were tested as model systems for vapor sensors that can monitor the level of humidity and carbon dioxide in a continuous stream of nitrogen. All coatings exhibited responses to water vapor on the order of kilohertz, while the responses to carbon dioxide were significantly (generally one order of magnitude) smaller. Interferences by the presence of both water and CO₂ on the SAW device sensitivity were observed with poly-(ethylenimine) (PEI) coatings as evidenced by the large extent of hysteresis. PEI coatings were also found to exhibit anomalous directions in frequency shifts when exposed to pulses of humidified CO₂, as did poly-(4-vinylpyridine) (PVP) coatings for lower humidity levels. ZSM-5 coatings, however, showed no evidence of such interference between water and CO₂.

Introduction

Interest in the use of surface acoustic wave (SAW) devices as chemical sensors has increased rapidly during the past decade. Wohltjen first reported this method of chemical detection in 1979,^{1,2} and in the years since, much effort by numerous groups all over the country, and indeed the world, has been spent in both the experimental and theoretical investigations of this technology.³⁻⁹ SAW devices belong to a class of chemical microsensors which owe their existence to the advent of microfabrication used three decades earlier in the electronics industry. Not only have they become popular due to their small size and sensitivity, but other characteristics inherent to these microsensors such as their ruggedness and low power consumption offer important advantages over traditional sensors in various environmental monitoring and process control applications. All of these properties combine to spearhead the constant drive to reduce the cost of chemical information, whose availability shall have profound implications for maintaining and improving quality in manufacturing, medical care, and the environment.

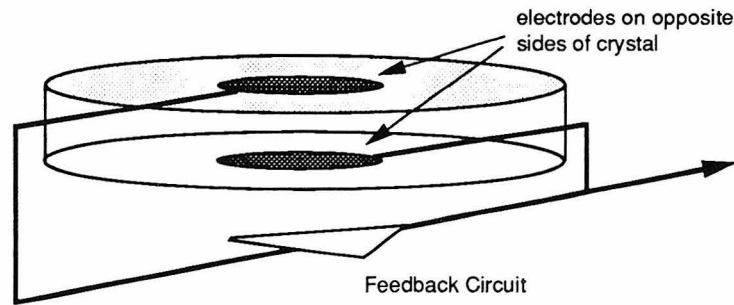
In the 1920s, Cady demonstrated that the converse piezoelectric effect could be exploited for the construction of very stable oscillator circuits.¹⁰ By applying an alternating electric field across a piezoelectric substrate, an alternating strain induces the crystal to oscillate at a particular resonant frequency and generates

acoustic standing waves. Changes in various properties of the crystal affected, for example, by its chemical or physical environment then act to perturb the acoustic waves such that a new resonant frequency is established. It is upon this transduction of mechanical vibrational energy to a detectable oscillating electrical signal that the SAW device relies in its detection of ambient chemical and physical conditions. In fact, because quartz crystals vibrate with minimal energy dissipation, they are nearly ideal oscillators and have been used widely in frequency control, filter circuits, and not surprisingly, chemical sensing.¹¹⁻¹³

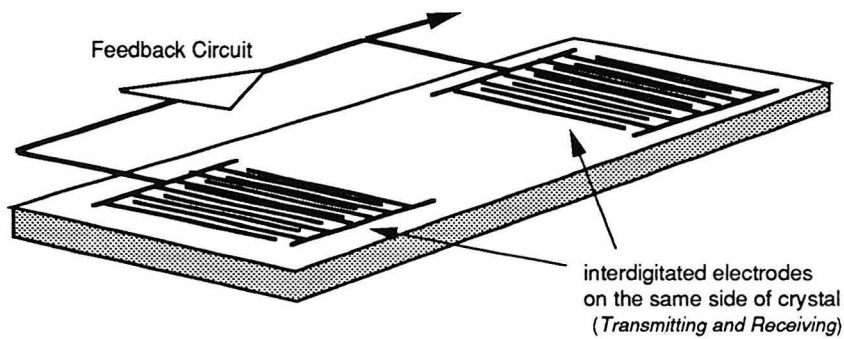
For chemical sensing, the actual perturbation of the acoustic waves usually results from the sorption of analyte. However, as quartz is fairly inert chemically, the SAW substrate itself is a poor sensor indeed. Selectivity is imparted only by introducing a chemically sensitive layer to the surface of the substrate, allowing a greater degree of interaction between the analyte and the acoustic wave. Because the SAW device ultimately relies upon the sensitivity of the surface waves to changes occurring in this thin surface film, this type of device has been used to determine such properties as polymer/vapor sorption thermodynamics and kinetics,¹⁴ adsorption/desorption isotherms,¹⁵ and pore size, surface area, and vapor diffusivity.^{16,21} The issue in chemical sensing with quartz-based SAW devices, then, is the development and design of coating materials that enable them to successfully probe the analyte of interest in a selective manner.

The concept of using a resonant piezoelectric device to measure the deposition of material onto the device surface was first reported by Sauerbrey in 1959 with his studies of the mass sensitivity of bulk acoustic wave (BAW) crystal resonators.¹³ This particular mode of oscillation occurs with the generation of standing waves across the bulk of the crystal. However, as the perturbation of these waves, in this

case material deposition, is restricted to the crystal surface, BAW resonators only achieved modest sensitivity levels. With King's introduction in 1964 of applying a chemically sensitive coating to the crystal surface,¹⁷ the idea of the chemical sensor was born and continues to be an active area of research today.



(a) a typical BAW device



(b) a typical SAW device

Figure 1. Comparison of a typical bulk acoustic wave device (a) and a typical surface acoustic wave device (b).

SAW technology was made possible in 1971 when White and Voltmer developed the lithographically patterned interdigital electrode.^{18, 19} Rather than being on opposite sides of the resonating crystal, as is the case with BAW device electrodes, the interdigitated electrodes of the SAW resonator lie on the same side of a crystal surface as illustrated in Figure 1. This particular arrangement allows surface waves to be launched by one set of electrodes and then converted back into an electrical signal by another on the same surface. There are, however, several modes of oscillation that can be excited, each with their corresponding wave forms. Figure 2 shows some of the types of elastic waves that can be generated, including

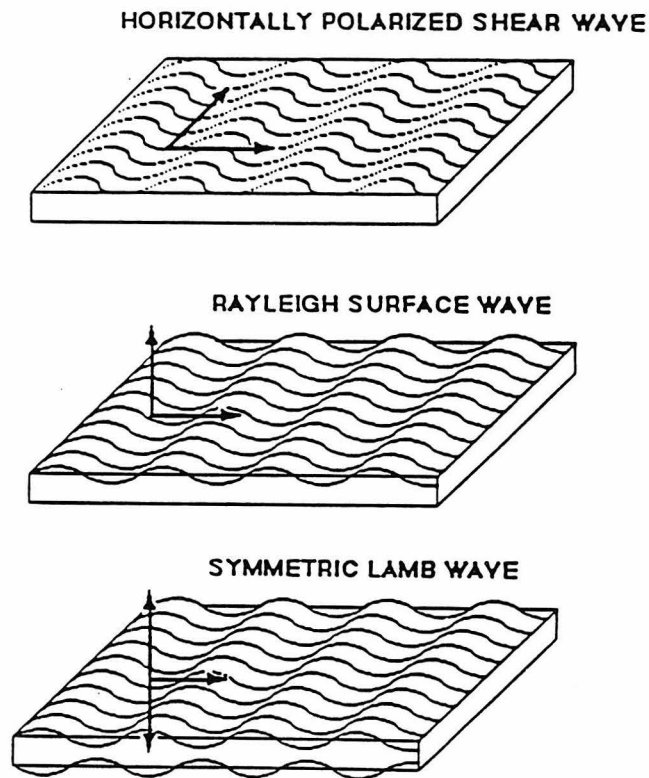


Figure 2. Different modes of acoustic wave oscillations.

the horizontally polarized shear waves, Lamb waves, and Rayleigh surface waves. While each wave has distinct advantages for specific applications, the Rayleigh surface acoustic wave is unique in that the crystal lattice displacement is confined to within a few wavelengths of the surface making it the optimal choice for studying surface phenomena. Wave formation depends largely on physical properties of the crystal and its exposed face, i.e., the symmetry group and the angle of cut, as well as the particular configuration of the electrodes. This project focuses on SAW technology based on Rayleigh surface waves.

Theory of SAW Device Operation

SAW chemical sensors often use a configuration that consists of a set of lithographically patterned interdigital electrodes (IDTs) deposited onto the surface of an optically smooth piezoelectric substrate. When a time varying potential is applied to the *transmitting* set of IDTs, a Rayleigh wave is launched that propagates along the device surface. This surface wave is converted back into an electrical signal by a second set of *receiving* IDTs. This particular configuration of electrodes is commonly referred to as a delay line. Although both the amplitude and the velocity of a Rayleigh wave are readily detectable for sensing purposes, it is usually the latter that can be monitored with the highest precision.²⁰ When such a delay line is used as the feedback element in an oscillator circuit, the frequency of the circuit is linearly related to the surface wave velocity. This relationship is given by Equation 1.

$$f = \frac{(2n\pi - \phi_e)V_s}{\ell} \quad (1)$$

Here, n is an integer, ϕ_e is the electrical phase shift of the amplifier circuitry, V_s is the surface wave velocity, and ℓ is the acoustic path length of the delay line. In practice, n is restricted to a small number of values (ideally, one value) by the limited bandwidth of the interdigital transducers and RF amplifier. The RF amplifier is necessary to overcome a typical 10 to 20 dB insertion loss of the delay line.²⁰

Chemical detection is accomplished when sorption of analyte species from the vapor phase onto the surface layer perturbs the velocity of the acoustic waves so as to produce a detectable response in the frequency. For an isotropic, non-conducting coating applied to a SAW device surface, the frequency shift can be described by the following relationship derived from the perturbation theory of Auld^{21,22}:

$$\Delta f = (k_1 + k_2) f_o^2 h \rho - k_2 f_o^2 h \left(\frac{4\mu}{V_s^2} \right) \frac{\lambda + \mu}{\lambda + 2\mu} \quad (2)$$

where Δf is the observed SAW oscillator frequency shift, k_1 and k_2 are material constants for the piezoelectric substrate, f_o is the unperturbed resonant frequency of the SAW oscillator, h is the coating thickness, ρ is the coating density, μ is the coating shear modulus, λ is the coating Lamé constant, and V_s is the Rayleigh wave velocity on the piezoelectric substrate (3158 m/sec for ST-cut quartz).²¹ Beyond the restriction on the type of coating material mentioned above, this equation is only applicable for very thin films that are less than approximately 0.2% of the acoustic wavelength. The second term of Equation 2 contains all the elastic parameters characteristic of the coating material. For most organic polymer coatings, the shear

modulus is significantly smaller than the Rayleigh wave velocity, and the second term can usually be neglected without introducing much error. Under these conditions, then, Equation 2 can be approximated by

$$\Delta f = (k_1 + k_2) f_o^2 h \rho \quad (3)$$

The product of coating thickness and density $h\rho$ merely corresponds to the mass of chemically sorbed species per unit area. Thus, given a constant surface area on the SAW device, a shift in the oscillation frequency should be linearly related to mass loading. Since both k_1 and k_2 for ST-cut quartz are negative ($-8.7 \cdot 10^{-8} \text{ m}^2\text{s/kg}$ and $-3.9 \cdot 10^{-8} \text{ m}^2\text{s/kg}$, respectively), an increase of mass on the surface corresponds to a negative shift in frequency.²⁰

Issues in Selective Coatings

As the sensitivity of the SAW device is entirely determined by the ability of the coating layer to either adsorb or absorb the chemical species of interest and concentrate it onto the device surface to the extent that a shift in frequency can be induced in the resonator, the design, synthesis, and evaluation of this sorbent coating for piezoelectric sensors is an active area of research. One of the issues that must be addressed is the nature of this vapor-coating interaction. Rather than being discrete, these energies of interaction extend widely over a continuous range. Practically, the weakest of these include van der Waals type interactions with bond energies less than 0.1 kcal/mol , while the strongest covalent bonds have energies exceeding 100 kcal/mol .

Experimental observables such as specificity, response time, and reversibility are generally highly dependent on the energy of sorption. Coatings exhibiting very strong covalent interactions with a few select vapors may be very specific in terms of its ability to detect the presence of these vapors, but these strong interactions are also not readily reversible. Thus, adsorption of vapor by covalent interactions can result in large accumulations of mass. Devices with these coatings may find applications as alarms to warn against a sudden increase or accumulation over time of certain undesired compounds, but they are inevitably precluded from use as chemical sensors in continuously monitored systems. At the other extreme are coatings with very weak interactions. These are highly reversible, but have a tendency to interact with numerous classes of vapors. This is where the advantages of shape selectivity can be exploited by using microporous zeolite coatings. Obviously, moderate ranges of vapor-coating interaction energies are a practical necessity for most applications to maximize both sensitivity and reversibility. Some well known intermediate energy bonds include hydrogen bonding, charge transfer complexation, and other donor-acceptor type interactions.²⁰

It is clear that the design of a chemically selective coating for sensing purposes is a very complicated problem owing to the rather primitive understanding of vapor-coating interaction chemistry. As theories pertaining to bulk phase chemistry continue to prove unsatisfactory in accurately describing or predicting similar behavior in thin films, new models are being developed using available physical and thermodynamic parameters.²³ Until such models are available, there are two important conceptual approaches to guide the design of such selective coatings, namely, the *dynamic adsorption concept* and the *solution concept*, as illustrated in Figure 3.

The *dynamic adsorption concept* generally applies to coatings that are hard and dense, and relies on the kinetic theory of gaseous adsorption as described by Langmuir in 1918.²⁴ This details a single parameter relationship between the number of molecules per unit surface area and a parameter called the *sticking time*, or the average time that a molecule remains sorbed on the surface. The latter is known to exhibit an exponential dependence on the energy of adsorption, but is in fact difficult to estimate accurately.

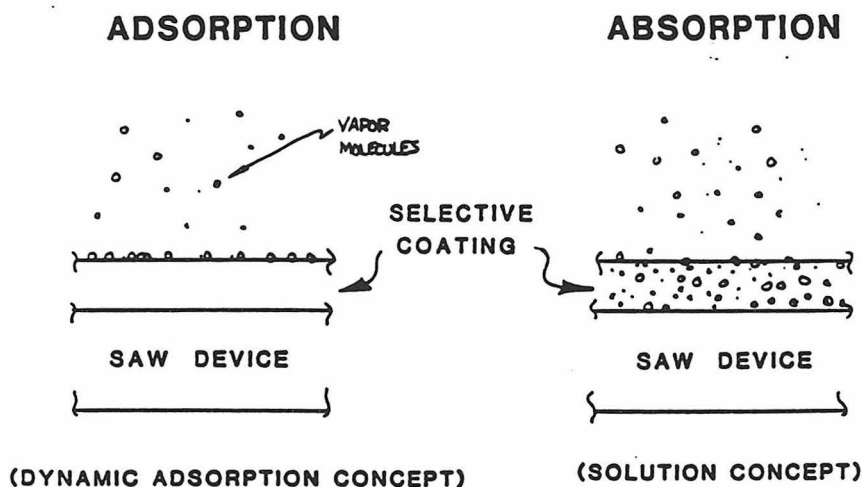


Figure 3. Two conceptual approaches to understanding vapor-coating interactions.

The *solution concept*, however, models the coating layer as a solvent and the vapor analyte species as the solute. Although this model has mostly been used to describe absorption of vapor into elastomeric organic polymers rather than

adsorption onto surfaces, it is also quite useful in the study of adsorption phenomena observed with porous and microporous inorganic solids such as zeolites. One important conclusion from this theory is that the sensitivity of the device increases as more coating is applied to the surface. This is true until the device becomes so heavily loaded with coating that the oscillator noise becomes excessive or the surface waves are dampened altogether. Another predicted correlation is the linear dependence of the frequency shift on the vapor concentration. Experimentally, however, linearity is only observed at lower concentrations.²⁰ Yet a third phenomenon that is predicted by the solution concept is diffusion effects. This is manifested as the response time behavior of the sorption process. Frye and Martin demonstrated the simple linear relationship between concentration (reflected by the frequency shift) and the square root of time for transient diffusion as described by Fick's Law.²⁵ Such techniques may prove to be useful in determining the effective diffusivities of species in thin films, which can differ significantly from that of bulk samples prepared from the same material.²⁶

Experimental Objective

This project focuses on the development of sensing technology to monitor ambient chemical environments. Of particular interest is the maintenance of artificial environments as part of the life-support capabilities of prolonged space travel. Although contaminants such as carbon monoxide, aromatics, ketones, aldehydes, and other halogenated hydrocarbons that may result from outgassing of electronic equipment also need to be addressed ultimately, the two immediate

concerns above parts-per-million levels are humidity and CO₂. Here, the objective is to synthesize coated SAW chemical sensors to continuously monitor humidity and CO₂ levels.

Experimental Methods

Materials

The 158 MHz dual SAW delay line oscillators (Figure 4), fabricated from aluminum IDT electrodes on polished ST-cut quartz substrates, were purchased from Microsensor Systems, Inc. Poly-(ethylenimine) (PEI, average molecular weight 1,800) and linear poly-(4-vinylpyridine) (PVP, average molecular weight 50,000) polymers that were used as coating materials were obtained from Aldrich and Polysciences, respectively. Chromosorb 102 (80/100 mesh) resin was used to fill the humidity saturator.

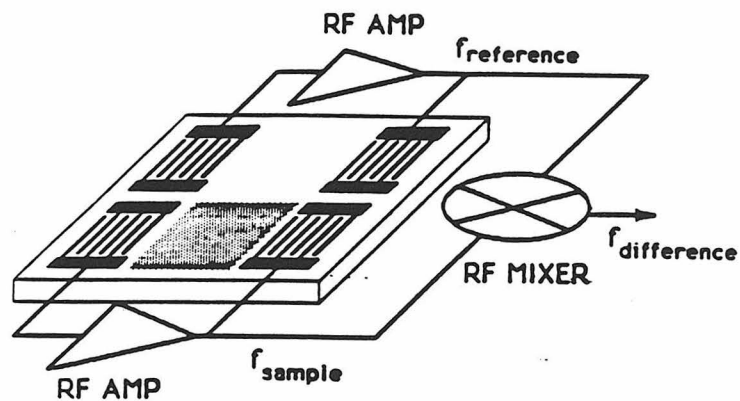


Figure 4. Dual SAW delay line sensor configuration.

Synthesis

The synthesis of nanophase pure-silica ZSM-5 crystals was based on the work of Zecchina *et al.*²⁷ One of the most common procedures employed to reduce the size of synthetic crystals is the utilization of a CSTR (continuously stirred tank reactor) under autogenous pressures rather than a batch reactor autoclave. The experimental procedure was as follows:

147.26 g of 15% aqueous solution of alkali-free tetrapropylammonium hydroxide (TPAOH, from Johnson Mathhey) was poured into a 100 mL Pyrex vessel containing 10.89 g of tetraethylorthosilicate (TEOS, 98% purity from Aldrich) with stirring. In this synthesis, TEOS was the only silicon source for the zeolite, while the TPAOH acted as the structure directing agent. This resulted in a two-phase solution that was gradually mixed upon further stirring. The solution was maintained at room temperature for 5 hours, heated to 343 K in an oil bath and subsequently kept at that temperature for an additional 5 hours. Finally, 50 mL of water was added and the resulting clear single-phase solution (molar composition 1 TEOS : 0.56 TPAOH : 80 H₂O) poured into a 250 mL autoclave. The autoclave was heated up to 448 K and maintained for 120 hours at that temperature with stirring under autogenous pressure. After cooling to room temperature, the white precipitate was separated from the mother liquor by vacuum filtration, washed free of excess TPAOH with distilled water, and dried at 393 K overnight. Total yield of white crystals was 2.2 g, or 60.9% based on TEOS. The uncalcined sample was used as made. Calcination was achieved by further heating of the sample at 813 K for 2 hours in air. The X-ray powder diffraction pattern and TEM micrograph of the crystallites, shown in Figure 5, both confirmed the crystal structure to be that of

ZSM-5 and established the crystal sizes to be fairly uniform on the order of 100 nm, respectively.

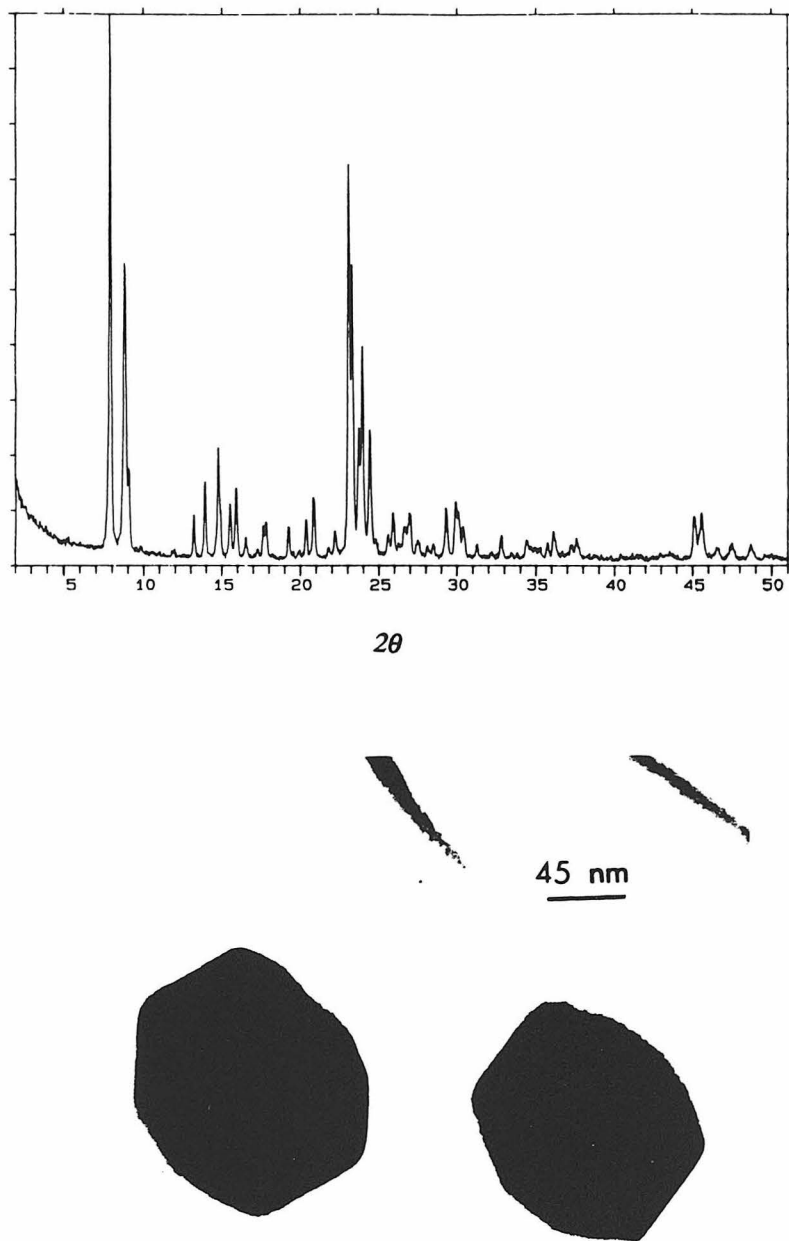


Figure 5. XPD spectrum and TEM micrograph of nano-phase silicalite ZSM-5.

Characterizations

SEM micrographs were obtained on a Camscan Series 2-LV scanning electron microscope using a 15 *kV* potential. To provide a conductive surface prior to microscopic examination, the samples were coated with gold using an argon plasma. TEM micrographs were obtained with a Philipps 301 transmission electron microscope using a 100 *kV* potential. X-ray diffraction (XRD) patterns were collected on a Scintag XDS-2000 diffractometer that is equipped with a liquid nitrogen cooled germanium solid-state detector using Cu-K α radiation. Film thicknesses were measured with a Gaertner Scientific Corp. model L116C ellipsometer. However, as a reflective surface is necessary to employ ellipsometry, measurements could not be performed on the actual SAW devices. Instead, films were generated on test grade silicon wafers using the same spin coating parameters and procedures as described in the *Coating Preparations* section. Film thickness measurements were taken at four to six locations over the silicon wafer surface, and the average value was reported as the film thickness.

Coating Preparations

All surface films were prepared by spin casting a solution (for organic polymer films) or suspension (for inorganic crystalline films) of the compound of interest onto one SAW device at *ca.* 3000 *rpm* with usually one drop from a transfer pipette. The coated SAW devices were then heated to 348 *K* in air for the films to cure and the volatile solvents to evaporate.

The organic solutions were prepared by simply dissolving the polymer in a volatile solvent—methanol for PEI and chloroform for PVP. In this study, 1.5 wt.% PEI and 2.8 wt.% PVP solutions were used. Preparations for the inorganic

zeolite-silica suspensions were based on the technique used by Bein *et al.*,²⁸ the principle being to finally embed the zeolite crystals in a polymerized TEOS matrix. This process is accomplished by suspending finely ground samples of zeolite crystals (*ca.* 0.3 to 1.0 g) in alcoholic solutions of TEOS. Initially, an alcohol-TEOS stock solution is made from a mixture of 61 mL of TEOS, 61 mL of ethanol (reagent grade), and 5 mL of 0.04 M HCl. 10 mL of this stock solution were then mixed with 1.0 mL of 0.05 M NH₄OH to form a silica sol. To a 2.5 mL aliquot of this silica sol was added 5 mL of ethanol to form the final suspension medium. In order to ensure the even distribution of crystals, the zeolite suspension was pulverized for approximately 3 to 5 minutes in an ultrasonic bath before application of coating. It is known that polymerization of TEOS usually occurs either via acid catalysis or base catalysis. However, as both acid and base are used in this procedure, it is not clear at which step the polymerization actually occurs. The rather small amount of HCl used in the stock solution may in effect be used to stabilize the mixture, while the larger portion of NH₄OH actually catalyzes the polymerization process.

Vapor Flow System

SAW devices were clamped into a stainless steel holder using small pressure clips and screws. A lid attached to this holder was fitted with inlet and outlet tubes to provide a vapor flow path. Vapor stream flow rates were regulated using mass flow controllers (Brooks 5850 and 5850E series) and calibrated using a volumetric soap-film flowmeter. All metal plumbing was stainless steel or brass connected with Teflon tubing. Distances between parts of the apparatus were minimized, and nitrogen was used as the inert carrier gas.

The method of generating water vapor used in PEI experiments (Figure 6) involved passing nitrogen gas through a glass saturator vessel filled with wet chromosorb resin. The relative amount of water vapor being introduced was determined by the saturator temperature, which was regulated by means of a circulating bath. Assuming the N_2 that was passed through the chromosorb resin is saturated, the amount of moisture was calculated based on the partial pressure of water at the measured saturator temperature. As the resonant frequencies of SAW oscillators have proven to be extremely temperature sensitive, humidified streams generated in this fashion were made to flow through a coil immersed in a water bath at room temperature before being introduced to the SAW devices. The limits of humidity achieved in this system were between approximately 17% and 100%.

A second method (Figure 7) of generating water vapor was to bubble the nitrogen carrier stream through a water bath maintained at a constant temperature. Control of the relative humidity was then accomplished by diluting this humidified stream with varying amounts of nitrogen downstream. When available, a chilled mirror was used to continuously monitor the total moisture content of the gas line. Typical ranges of humidity that were achieved with this system was approximately 5% to 30%. Although the system itself was capable of generating humidity levels of up to 100%, performance limitations of the chilled mirror restricted the maximum to approximately 30%.

The flow systems described above were also employed in the generation of dry CO_2 streams. With these gases, however, a commercial pressurized tank was used as the source. Again, the vapor content was controlled by dilution with the nitrogen carrier stream. Wet CO_2 streams were then generated by combining the CO_2 and the humidifying schemes in series. In all cases, the total volumetric flow

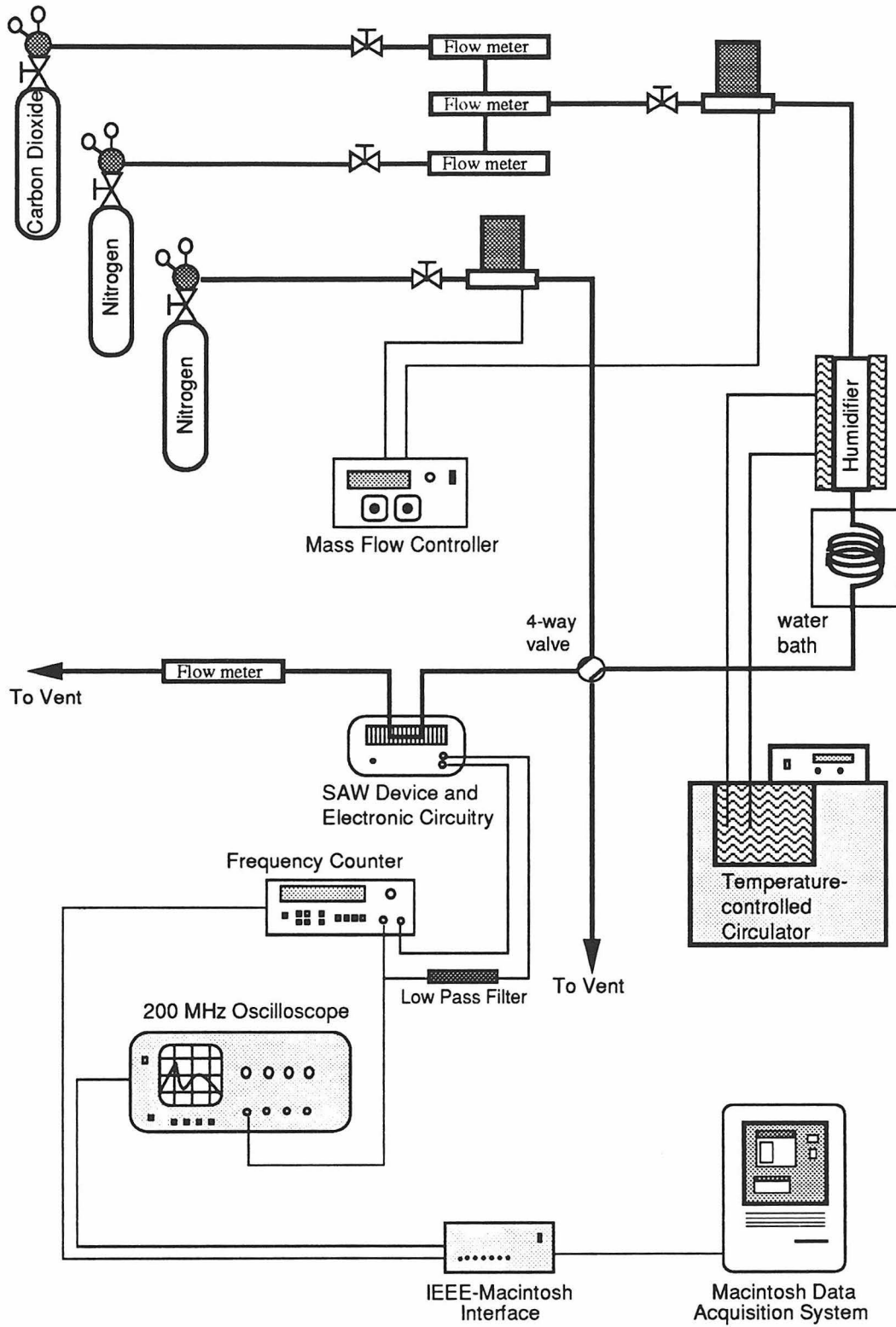


Figure 6. First experimental apparatus for vapor generation.

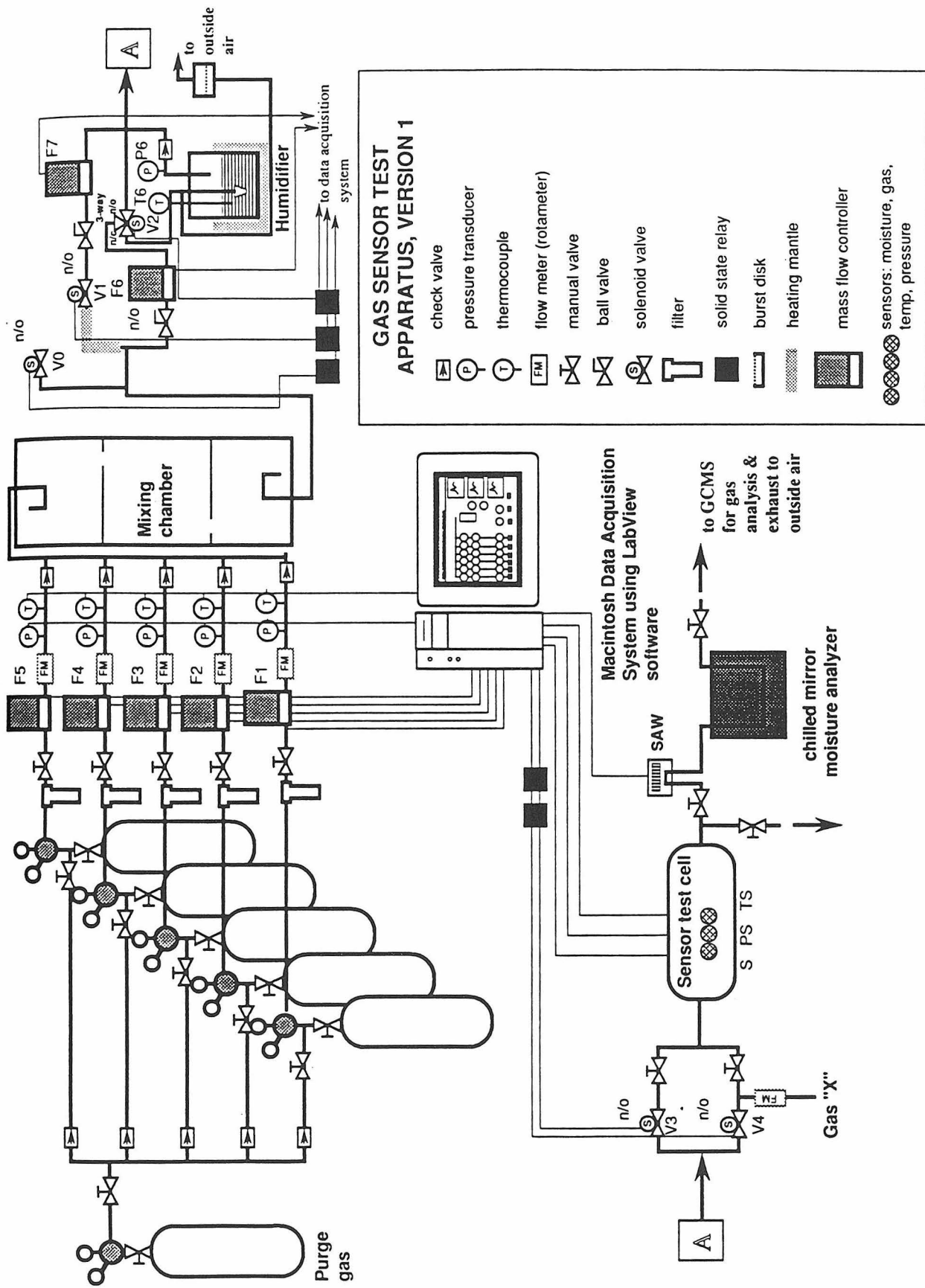


Figure 7. Second experimental apparatus for vapor generation.

rate was maintained at a constant value by adjusting the amount of nitrogen during experiments, usually ranging between 33 and 100 *mL/min*.

Results and Discussion

Surface Film Deposition

Poly-ethylenimine (PEI) and poly-4-vinylpyridine (PVP) films were spin cast onto the surface of the SAW device. It was found that spin coating produced relatively uniform film thicknesses within a radius of about 1 *cm* from the center of the circular test wafer for organic polymers. As the surface area of the SAW substrate is fixed, the amount of coating introduced corresponds directly to the thickness of the film, which can be controlled by parameters such as the viscosity of the sample solution and the spinning rate. The coatings should be applied over the IDT electrodes as well as the inter-electrode spaces to obtain the theoretical sensitivity derived for SAW devices.²¹ Coating thicknesses ranged from *ca.* 200 Å to 1500 Å for various test runs, but measurements within each test run deviated no more than approximately 100 Å .

ZSM-5 coatings were prepared in like fashion. Ellipsometry revealed great disparities in film thickness measurements on the same silicon test wafer. This was not completely unexpected though, as SEM micrographs showed the surface to resemble non-continuous domains of zeolite crystals embedded on the polymerized TEOS matrix. It was also found that applications of larger crystals of pure-silica ZSM-5 (*ca.* 1-3 μm) and sodalite (*ca.* 10-40 μm) resulted in the 158 *MHz* SAW device substrate losing its ability to oscillate. Signals from a SAW delay line feedback loop typically had amplitudes of 1.2 *V* peak-to-peak. After coating the

surface with these larger zeolite crystals, however, the amplitude of the oscillation decreased to below 100 mV , while the frequency counter failed to register any signal at all. One possible cause of this phenomenon could well be the destructive interactions of the surface waves as they are severely scattered by domains of large crystals. Signal amplitudes from PVP and PEI coated devices suffered nearly no dampening effects, whereas signals from the nanophase pure-silica ZSM-5 coating decreased the signal amplitude to the $0.8\text{-}0.9\text{ V}$ level.

This trend underscores the importance of having uniform films for detection purposes; it goes beyond the convenience of correlating data with available theory into a matter of experimental practicality with electronic detection. One method of avoiding the problems that embedded zeolite coatings appear to present is to epitaxially grow these inorganic films onto the surface of the SAW substrate, rather than spin casting sample suspensions. The advantage with this approach is that it offers a significantly higher degree of control over the uniformity of the chemically selective film.

Device Design

The uncoated SAW devices used in this study have a nominal frequency of 158 MHz . Many sensor applications use a dual SAW delay line configuration similar to that depicted in Figure 4, where two sets of transmitting/receiving IDTs are lithographically patterned onto the same oscillator surface. One delay line is coated with the chemically selective film, while the other is left uncoated. The frequencies of the two delay line oscillators are mixed electronically to provide a frequency equal to the difference of the two oscillator frequencies.²⁰ In principle, frequency drifts effected by ambient temperature fluctuations experienced by the

SAW device are compensated by this scheme. However, as the total active area of the device surface is only 0.08 cm^2 , coating only half of this area by conventional spin coating methods is not possible. Instead, two separate SAW devices were used. If the uncoated SAW substrate is not sensitive to the analyte in the gas stream, then it is possible to insert this reference device into the flow stream as an additional compensatory measure for pressure fluctuations as well. Otherwise, a sealed reference SAW device is used instead. Although it has been found that gradual pressure changes in the gas line has little effect on the SAW frequencies, engaging and switching of certain valves in the manifold produces transient shock waves that occasionally appear as spikes in the signal. While the strategies described above do minimize temperature and pressure effects significantly, problems with signal drift is not always eliminated.

SAW Sensor Performance with Organic Polymer Coatings

A typical SAW sensor response is illustrated in Figure 8. In this case, a poly(ethylenimine) (PEI) coated 158 MHz dual SAW device (average film thickness 272 \AA) was exposed to repeated pulses of $18.5 \mu\text{g}/\text{m}^3$ water vapor at room temperature. As the sensor is exposed to humidified pulses in the vapor stream, water is sorbed into the polymer coating layer, thereby increasing the mass loading on the SAW oscillator. The frequency of the *sample* SAW device (the device coated with the chemically selective film) is initially less than that of the *reference* uncoated SAW device due to application of the PEI coating. Vapor sorption then further decreases the oscillation frequency of the *sample* SAW device. As the *reference* SAW device is unchanged, however, this process increases the absolute difference frequency, Δf or $|f_{\text{reference SAW}} - f_{\text{coated SAW}}|$, which is the ordinance in

this plot. Upon removal of the vapor, the frequency difference decreases and returns to the original baseline value. Such reversibility of response is essential for continuous monitoring applications. The repeatability of response is quite good.

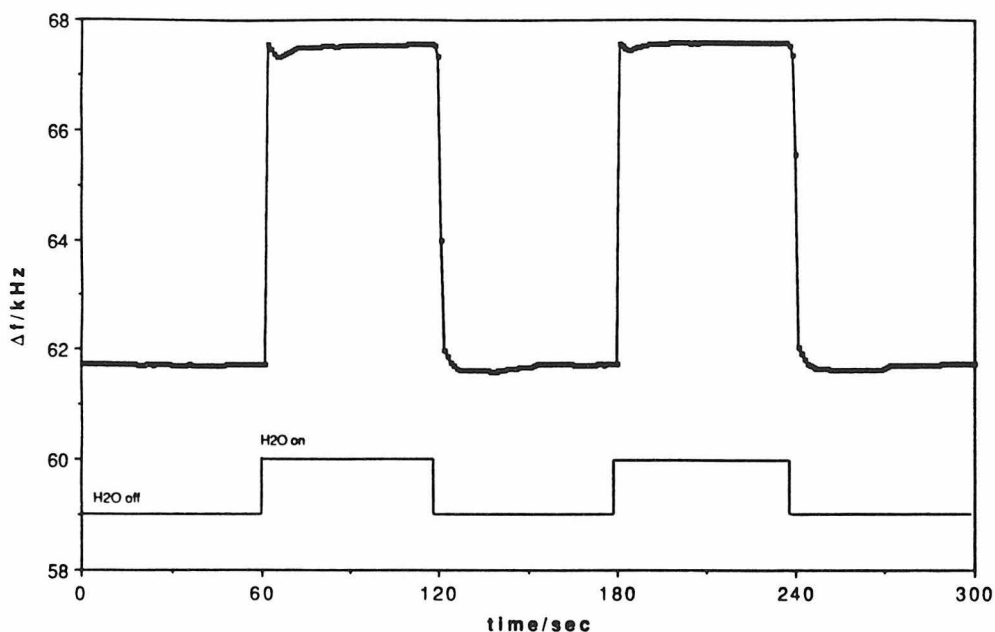


Figure 8. Typical response of a PEI coated SAW sensor to consecutive pulses of water at room temperature.

The response time of the sensor is extremely rapid in this case, achieving the equilibrium value in approximately 10-15 seconds. Generally, the sensor response time is concentration dependent, ranging from about 10 seconds for higher concentrations as reported above to about 2 minutes for lower concentrations. Many other factors such as detector cell dead volume, coating morphology, coating glass transition temperature, and thickness may also influence the response time.²¹

A portion of the sorption isotherm for the water/PEI system is shown in Figure 9. The best fit for this range of relative humidities appears to be a quadratic one. However, as it is known that the frequency response must converge to zero as the relative humidity approaches zero, it is not unreasonable to extrapolate a curve

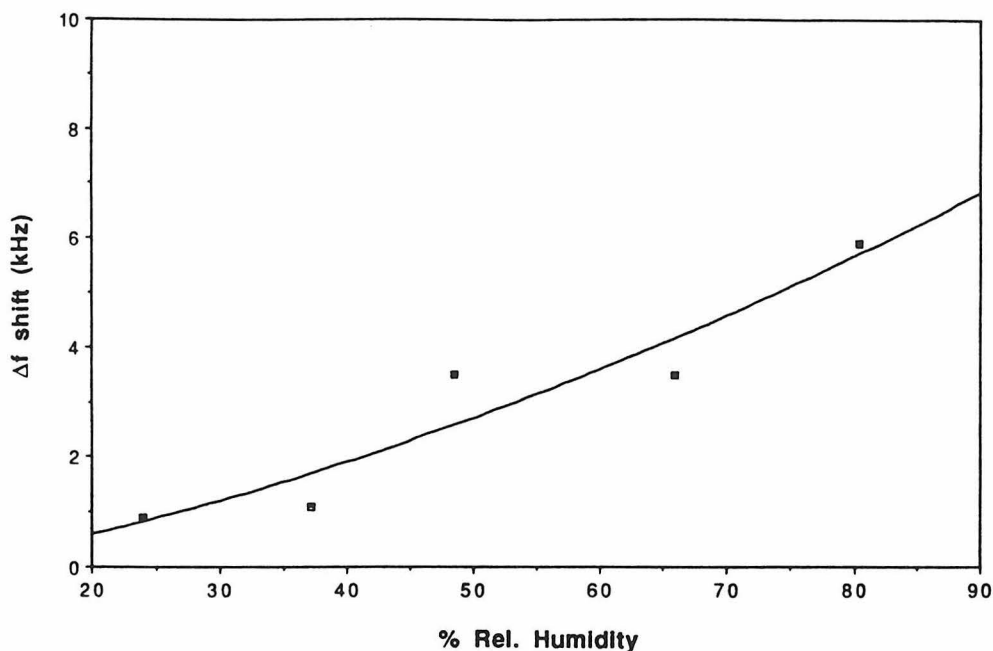


Figure 9. Sorption isotherm for water vapor on PEI coated SAW sensor at room temperature.

similar to the type III adsorption isotherm shown in Figure 9. Type III isotherms are characterized by their being convex with respect to the pressure axis. This may suggest the sorption process to be cooperative in nature; namely, the more molecules that are already sorbed, the more further sorption is enhanced. On *a priori* grounds it would seem that the attraction of adsorbate molecules for each other exceeds their attraction for the adsorbent. In light of this, the fact that this vapor-coating system exhibits such behavior is not surprising, as water is capable of forming hydrogen bonds. However, more data is necessary before any firm conclusions can be made.

Another important feature of SAW devices that is well illustrated by this example is the high level of detectability that can be achieved. Noise levels of uncoated devices do not usually exceed ± 16 Hz, and that achieved in this experiment is no more than ± 25 Hz. This gives a signal to noise ratio on the order

of 500 to 1. Equation 3 predicts that a typical ST-cut quartz SAW vapor sensor operating at 158 MHz with an active surface area of 0.08 cm^2 will produce a frequency shift of about 400 Hz per nanogram of mass loading. This would suggest that the detection limit for moisture attainable with a PEI coated SAW device would be on the order of 100 picograms.

Figure 10 shows the response of a PEI coated SAW device to dry CO_2 . Firstly, it is clearly evident that the sensitivity of PEI to CO_2 is much lower than that for water. The signal produced by the 1.8% CO_2 stream is on the level of about 500 Hz. Secondly, it can be seen that the desorption process is extremely slow, as the removal of CO_2 affects almost no response. Rather, the SAW device maintains the original frequency shift, albeit with a slow drift, until the second pulse further produces a small shift much like that produced by the first.

Previous studies have demonstrated the sensitivity of PEI coatings to water vapor,²¹ but none have tested the possible interferences that the presence of other gases may have. Figure 11 shows the effect that CO_2 has on the detection of water vapor. A stream of humidified nitrogen (at approximately 65% relative humidity) is used to establish a baseline response in the SAW device. Upon introduction of 2% CO_2 at the same H_2O concentration (the amount of nitrogen being reduced to maintain a constant total flowrate), the SAW device responds quite rapidly in the initial phase, and then slows considerably after 20 to 30 seconds as it reaches the equilibrium value. A very striking feature of this response, however, is the fact that the frequency shift is negative, corresponding to a decrease in mass loading.

Further experiments using a gravimetric technique confirmed the decrease in mass as CO_2 is introduced to a humidified nitrogen stream. A similarly coated SAW device was placed on Cahn balance fitted with gaslines to duplicate the same

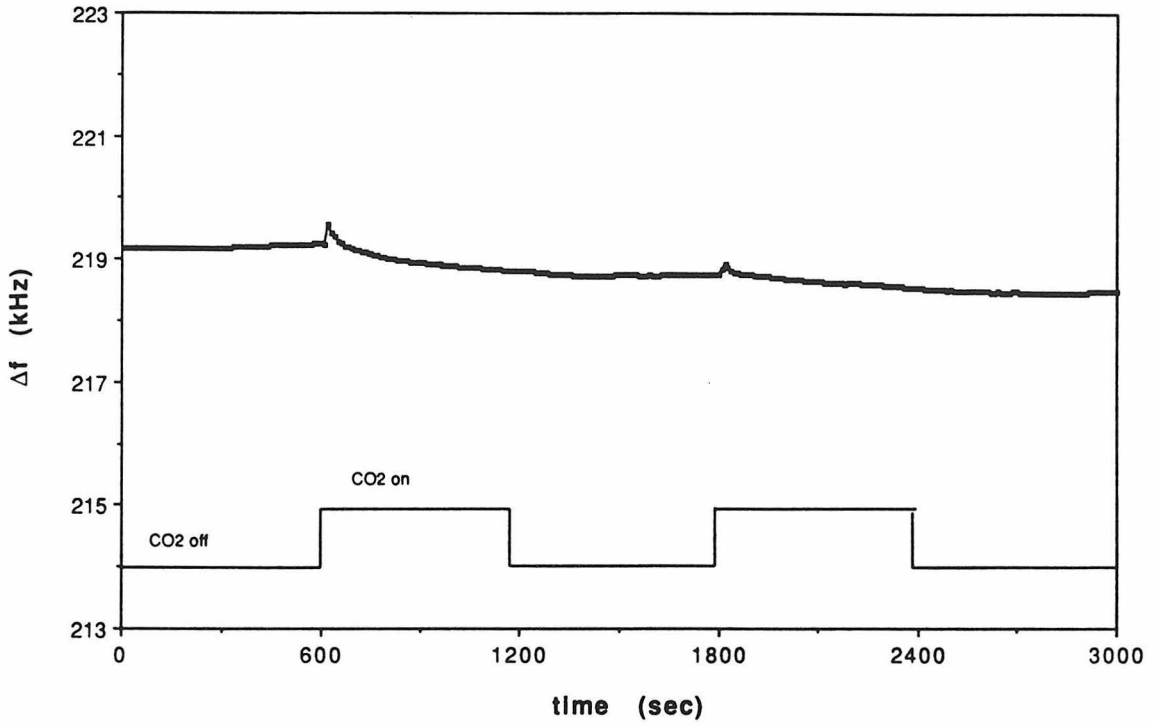


Figure 10. Response of PEI coated SAW to pulses of 1.8% dry CO_2 .

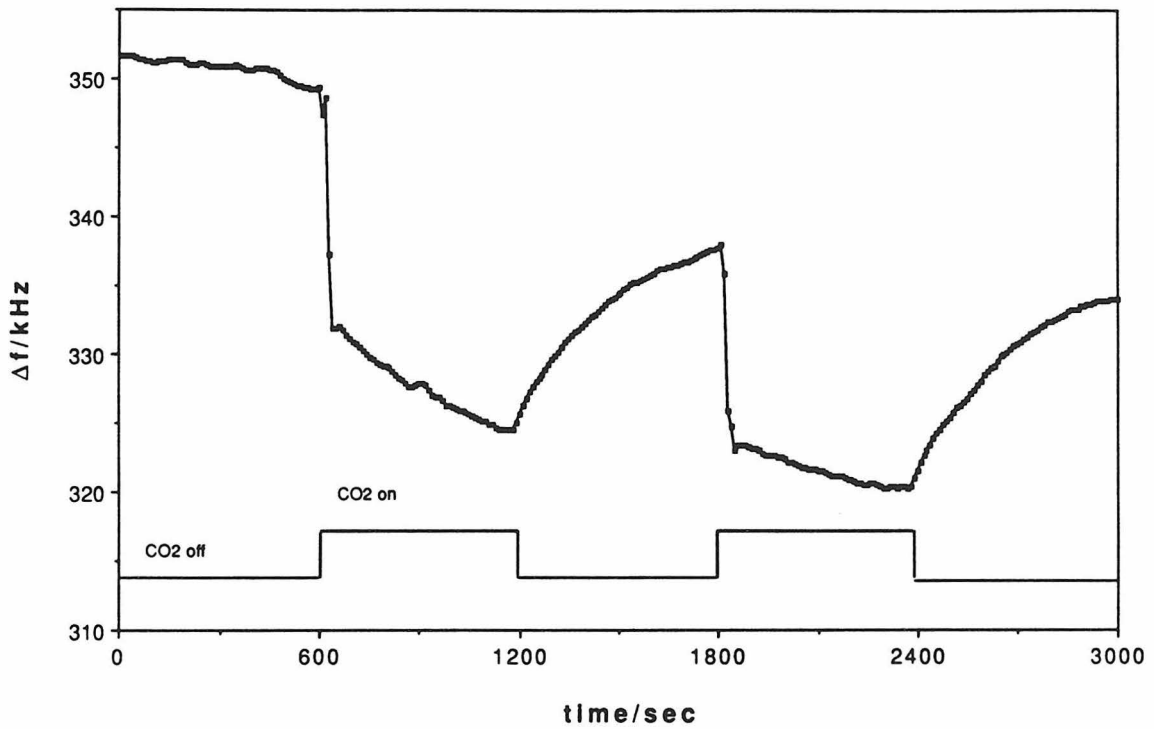


Figure 11. Response of PEI coated SAW to pulses of 2% wet CO_2 .

flow conditions as described above. Application of a greater amount the polymer was necessary to induce a response on the Cahn balance as its sensitivity was on the order of $0.1 \mu\text{g}$. When CO_2 was introduced to a previously established humidified stream (again, the amount of nitrogen adjusted to keep a constant total flowrate), the mass did indeed decrease. Upon removal of CO_2 from the stream, however, the balance returned to its original equilibrium baseline value.

This phenomenon can be explained in terms of the possible absorptive nature of the vapor-coating interaction of water and PEI using the solution concept. It is known that most organic polymers are physically elastic, and this property allows the sorbing vapor molecules to diffuse below the surface into what are commonly referred to as void spaces. For a given humidity level, equilibrium is established between the water molecules absorbed in these void spaces and ambient vapor molecules according to some effective partition coefficient. With the introduction of CO_2 (2% in this case) in the humidified stream, however, carbonic acid molecules begin to form either in the vapor phase or in the quasi-liquid phase within the void spaces after adsorbing and diffusing into the PEI film. This can significantly alter the pH of the absorbed "solution" in a manner that increases the polymer density and, hence, decreases the void volume. As the polymer responds in this fashion, its capacity for absorption likewise decreases, and water, CO_2 , and/or carbonic acid molecules are forced out of the surface film, thus resulting in the observed negative mass loading effect. A direct consequence of these changing polymer elastic properties can conceivably result in the observed hysteresis of the SAW frequency response after CO_2 has been switched off. While gravimetric analysis with the Cahn balance shows that mass loading returns to its original baseline rapidly, the SAW frequency exhibits a high degree of hysteresis, taking a significantly longer

time to reverse only about half its initial change. This would suggest that elastic changes may have occurred to such an extent that precludes the direct use of Equation 3. Rather, a deeper understanding of how elastic properties are affected by sorption processes is necessary to fully take advantage of the more complete description provided by Equation 2.

In light of the interference behavior between water and CO₂ which can possibly be attributed to the effects of carbonic acid, poly-4-vinylpyridine (PVP) was chosen to be tested with the water/CO₂ system. As pyridine has an *sp*²-hybridized nitrogen within an aromatic ring, PVP is likely to be much less basic than PEI, which has aliphatic amine groups. This should minimize the interactions (manifested as a negative Δf response and hysteresis) that were proposed to occur between PEI and carbonic acid.

Figure 12 shows the response of a PVP coated SAW device to pulses of varying humidity levels. It is evident that the response in the range of 10% to 25% relative humidity is fairly linear. However, humidity levels below about 8% induced a negative frequency shift. Since the analyte has not been changed, it is not likely that the same explanation used for PEI can be applied here. But it remains unclear what factors other than the polymer elastic properties and mass desorption may contribute to a negative frequency shift.

To dry CO₂, PVP showed almost no response, as frequency shifts consistently remained below 100 Hz for CO₂ levels of up to 6% by volume. Given the similar response of PEI to dry CO₂, this result was not exceptional. What was significantly different, however, was PVP's response to pulses of wet CO₂. Not only did PVP remain relatively insensitive to the presence of up to 20% CO₂ by volume, but its response to water was also unchanged. This absence of

interference between CO₂ and water was indeed a remarkable departure from that observed with PEI, which all but precluded its use in continuous monitoring systems. PVP would then be a likely candidate for a SAW coating that can be used as a humidity sensor in environments where variable concentrations of CO₂ may be encountered.

SAW Sensor Performance with Inorganic Zeolite Coatings

Zeolites have long been known for their molecular sieving properties that are a consequence of crystalline pore structures with pore diameters in the range of molecular dimensions. It is the combination of the mass sensitivity at the picogram level of SAW oscillators with the molecular shape and size selectivity of zeolites that present a promising future for such microporous films in molecular recognition and interfacial chemistry. The microporous framework of the zeolite films could endow the active region of the sensors with extensive surface area and volume for vapor sorption, and provide for molecular exclusion and recognition sites. Zeolite ZSM-5, for instance, has a high surface area to volume ratio (approximately 500 m²/g), and pore apertures on the order of 5.3 to 5.6 Å. In addition to its molecular sieving abilities, zeolites can be tailored chemically to have specific types of adsorbate-adsorbant interactions. For example, the presence of cage cations such as sodium can participate in dipole-dipole or dipole-quadrupole interactions, while ion exchanging these cage cations with protons forming silanol groups in the porous network can enhance adsorption of hydrophilic species. Use of electronically neutral templating agents and careful choice of synthetic conditions can result in zeolites with minimal crystal defects, and these materials are extremely hydrophobic. Because of its inorganic crystalline nature, zeolite films are also

much less susceptible to significant elastic changes that have been observed with the organic polymer films. Additionally, zeolite films offer extremely high thermal stability (greater than 770 K)²⁸ and chemical resistance.

In this study, zeolite ZSM-5 coated SAW devices were exposed to a variety of analytes in the vapor stream. Figure 13 shows a typical frequency response of TEOS-embedded, calcined, pure-silica ZSM-5 to pulses of varying relative humidities. Comparison of the isotherms obtained for calcined and uncalcined ZSM-5 coatings (Figure 14) reveals that the two are qualitatively different. The uncalcined ZSM-5 crystals have essentially all of the porous network blocked with templating molecules used in the original synthesis. Thus, the observed response of the uncalcined ZSM-5 coated SAW device can only be attributed to adsorption occurring on the TEOS matrix and the crystal surface. This is manifested in the near linearity of the isotherm, as the amount of water adsorbed increases in proportion to the amount of water vapor present in the nitrogen stream. The adsorption isotherm of the calcined ZSM-5 coating, however, shows a region where a preponderance of water vapor adsorption occurs. Following this region, the first derivative of the adsorption curve begins to taper off, approaching a finite value. This behavior is quite typical of type I isotherms, often observed for adsorption on microporous solids.

In very narrow pores such as those found in silicalite ZSM-5, the forces of attraction will be much stronger than on an open surface, because of the overlap of the fields from neighboring regions of the walls. This intensification of the field will distort the isotherm, in the sense of increased adsorption, from the course it would have had on an open surface of the same material. Indeed, some workers in this field hold that the effect will be to increase the heat of adsorption in the second

Figure 13

Adsorption of H₂O on Calcined ZSM 5 Coated SAW

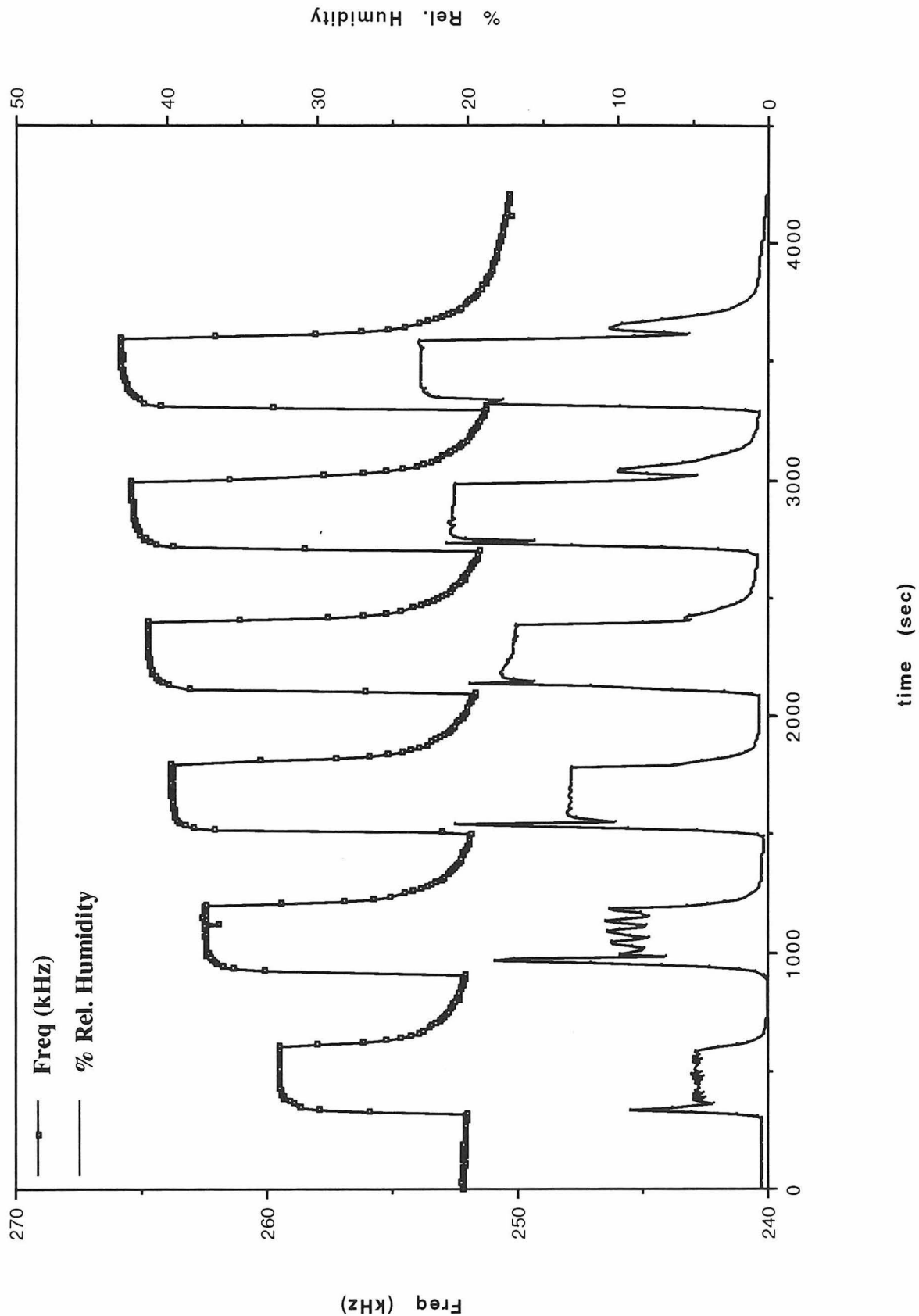
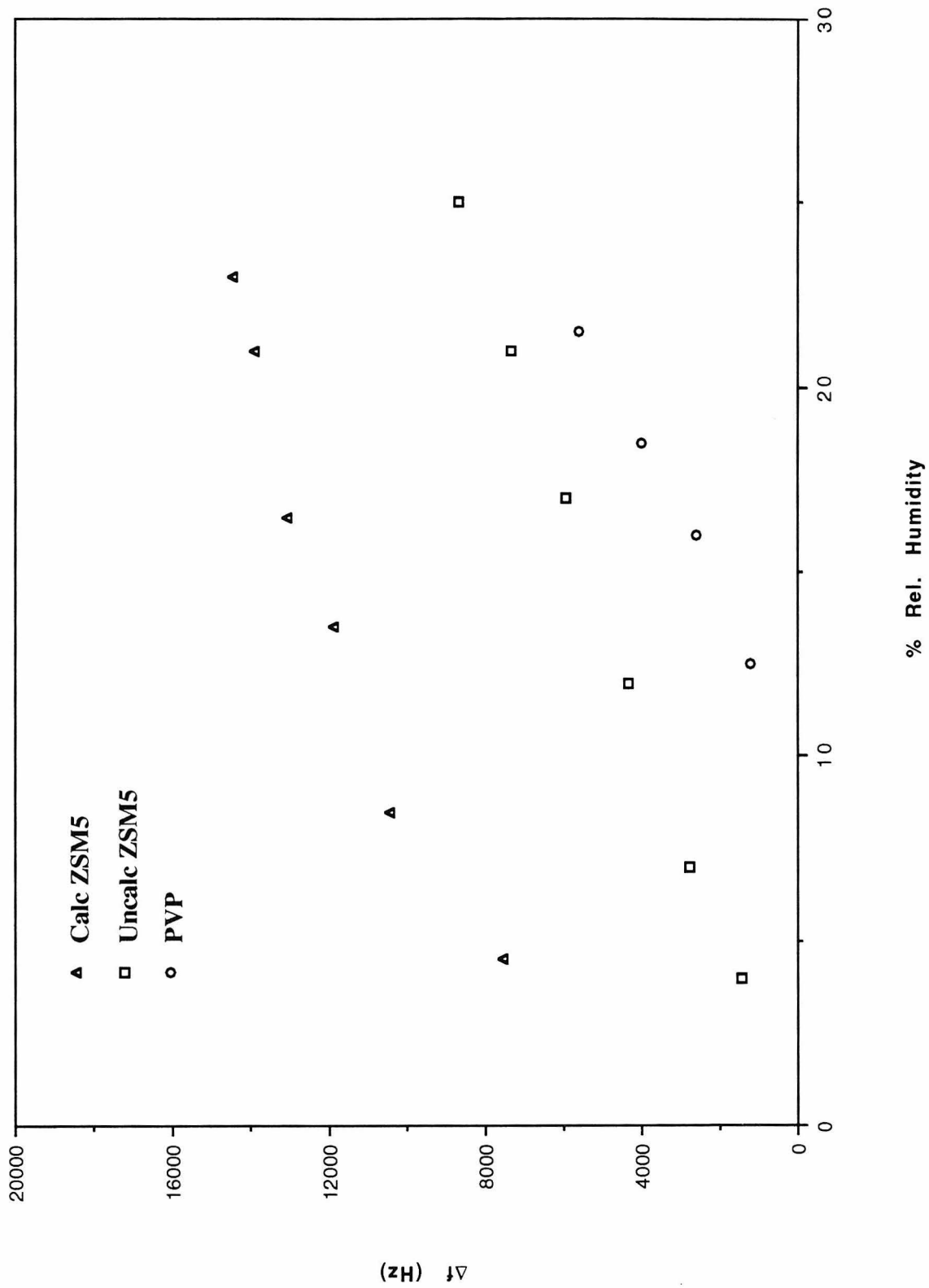


Figure 14

H2O Adsorption Isotherms

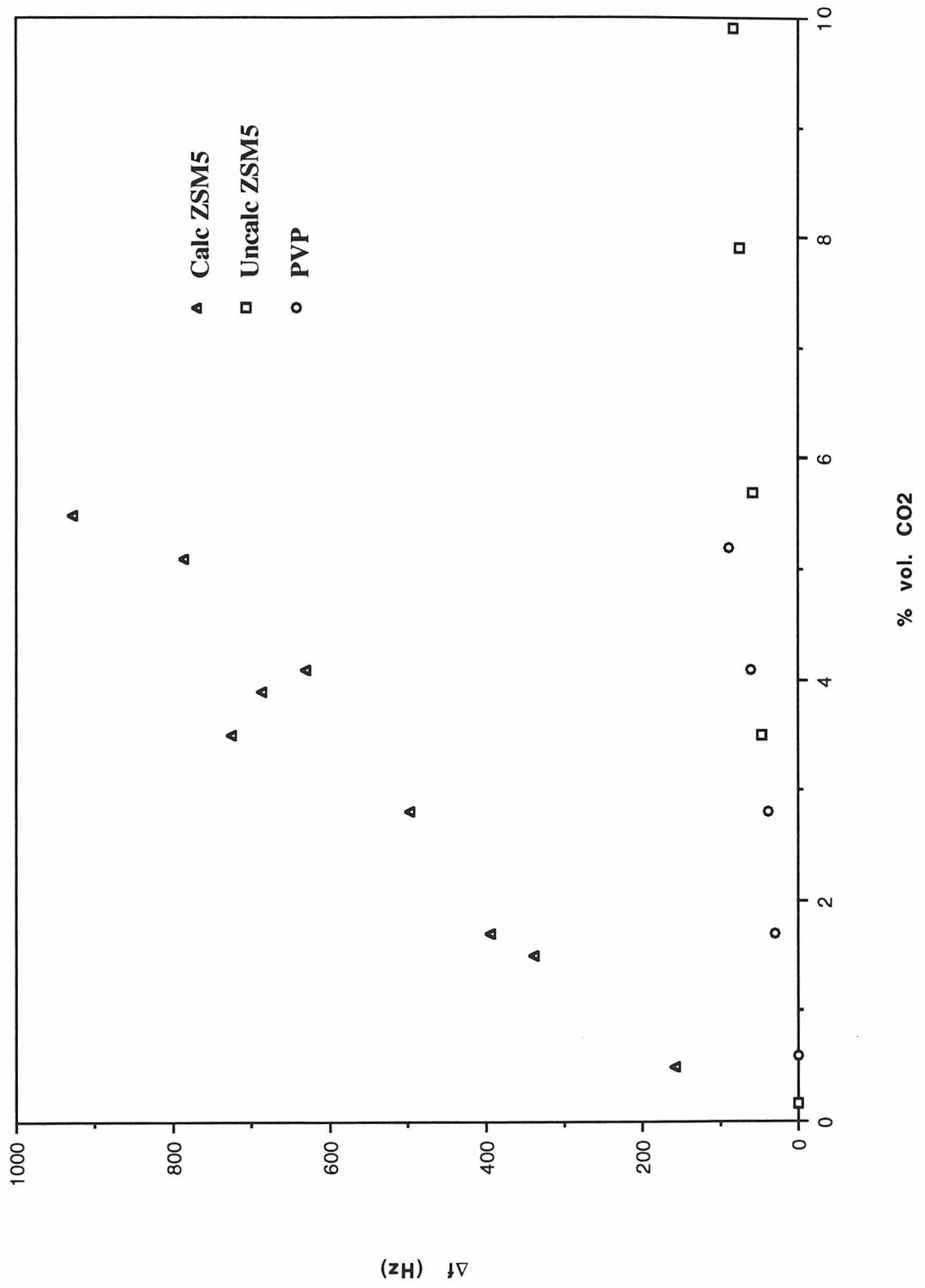


and possibly higher layers to such an extent that the sharp distinction between the first and higher layers is blurred.²⁹ There would then be no point on the isotherm that clearly corresponds to the filling of a monolayer. However, as there is no method to faithfully reproduce the coating of precise amounts of crystals via spin casting, or calcination of the coated zeolite films without inflicting damage to the SAW devices, quantitative conclusions about the relative amounts being adsorbed by the surface as opposed to the porous network cannot be made at this time. Even were faithful reproduction of coatings possible, it is difficult to speak of monolayers per se, as the pore apertures of ZSM-5 are only on the order of less than two molecular diameters for small analyte species such as water. Thus, with one molecule of the adsorbed species possessing the ability to obstruct the pore almost entirely, the idea of a monolayer loses its meaning altogether.

CO₂ adsorption isotherms are shown in Figure 15. One striking feature is that the sensitivities of all the films tested are several orders of magnitude greater for water vapor than they are for CO₂. Although silicalite ZSM-5 is commonly referred to as a hydrophobic zeolite because of its extremely high silica content, the synthesis procedure as described under *Experimental Methods* using TPAOH (tetrapropylammonium hydroxide) as the templating agent necessarily results in a minimum of one silanol group per cage. Additionally, the presence of crystal defects within the porous network further increases the number of silanol groups from hydrolysis of Si-O-Si bridges during synthesis. This can give rise to significant interactions with water molecules through hydrogen bonding. Usually, hydrophobic zeolites have water contents below 1% by weight. Figure 16 shows the thermogravimetric analysis profile of a sample of calcined ZSM-5. It is quite evident that the water content (as indicated by the extent of desorption at about the

Figure 15

Dry CO₂ Adsorption Isotherms



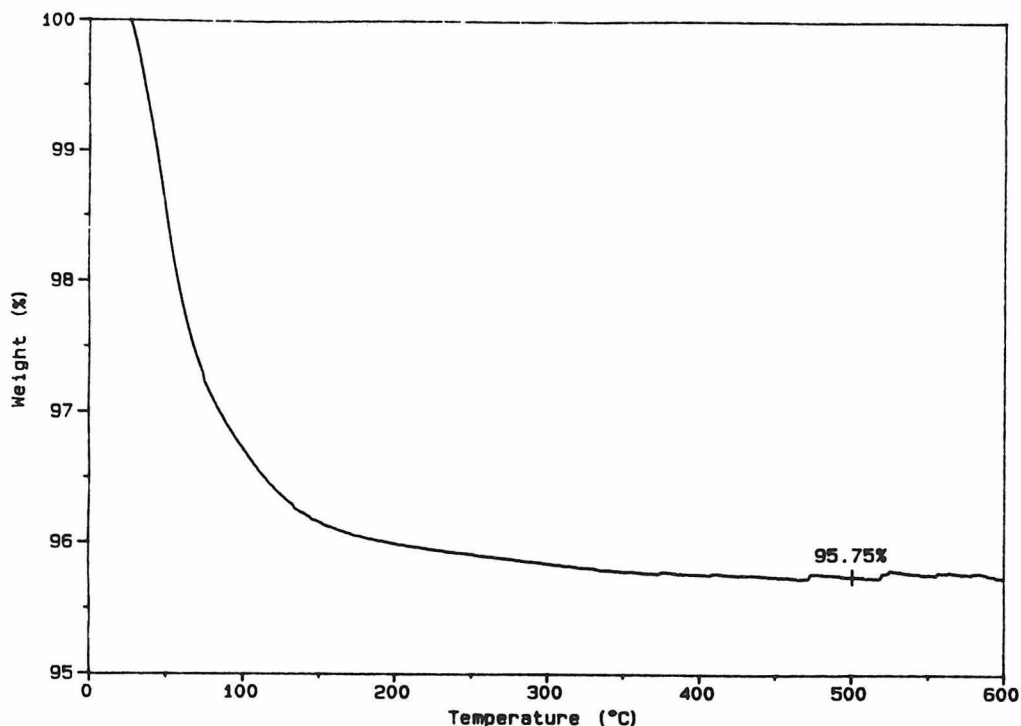


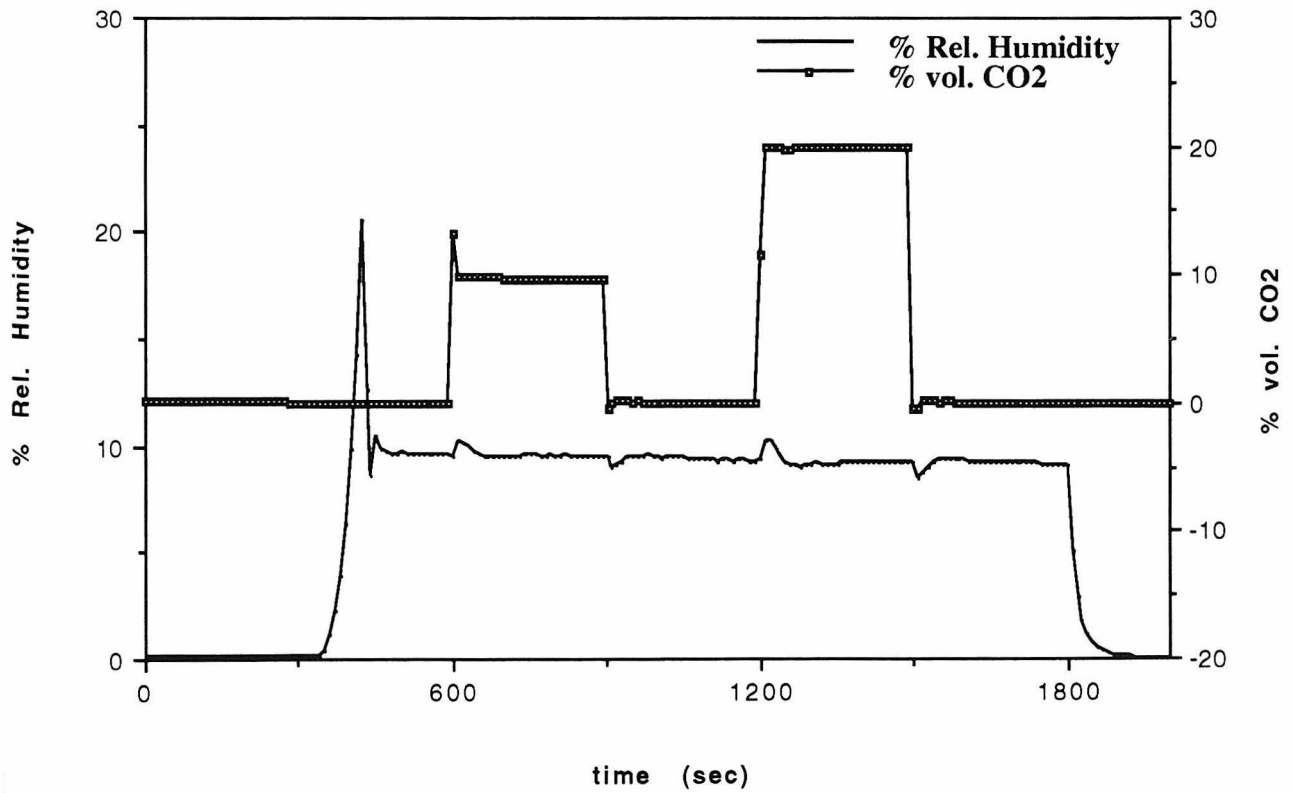
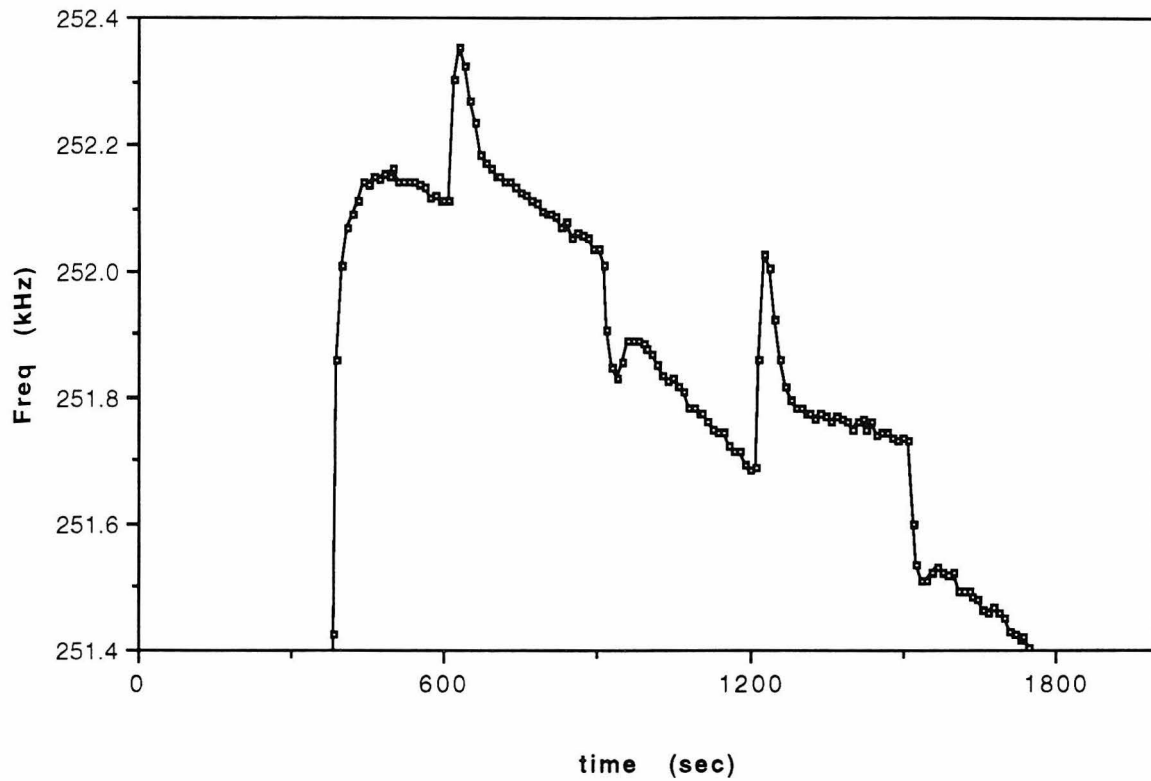
Figure 16. TGA spectrum of calcined silicalite ZSM-5.

100 °C mark) of this sample is rather high at approximately 4.25%, clearly indicating an abnormally high propensity to adsorb water.

As the isotherm for the uncalcined ZSM-5 coating from Figure 15 also shows considerable adsorption of water vapor, the amount of silanol groups on the crystal surface is likely to be quite substantial as well. However, as the response of the uncalcined ZSM-5 coated SAW device decreased more dramatically when the analyte was changed from water vapor to CO₂ than did the calcined ZSM-5 coated SAW device, this would suggest that the porous network of ZSM-5 is indeed more hydrophobic than the crystal surface/TEOS matrix composite. Thus, the density of silanol groups is possibly a great deal higher on the surface than in the channels and cages of ZSM-5.

While both organic polymer films exhibit effects that may be attributed to changes in elastic properties, none such phenomena are observed for the inorganic

Figure 17
ZSM-5 Coated SAW Response to Wet CO2



zeolite films. A very interesting consequence of this is the fact that little or no interference was found when both water vapor and CO₂ were present in the gas stream. The effects have been tested with both CO₂ pulses over a water baseline as well as water pulses over a CO₂ baseline. The former is illustrated in Figure 17. After the initial baseline with 10% relative humidity is established, pulses of CO₂ are introduced first at 600 seconds and again at 1200 seconds, the first being about 10% volume and the second about 20% volume CO₂. Although there is a drift of approximately 40 Hz/min in the baseline, it is clear that the responses from each analyte species simply “superimpose” themselves over each other, i.e., it is possible to see the CO₂ signals on top of the water signals and vice versa. This result would suggest the ZSM-5 coating to be a very likely candidate for sensing CO₂ in environments where the humidity is maintained at a constant level. Since the PVP film shows virtually no response to CO₂ in the presence of water vapor, an array of two SAW devices, one coated with PVP and another with pure-silica ZSM-5, could well provide a practical sensor for CO₂ in environments where the level of humidity is not constant. Such array configurations are presently the focus of a number of research efforts aimed at overcoming the difficult and time consuming task of developing adequate chemically selective coatings for one particular analyte.

Future Directions

There are several methods of overcoming the problems associated with quantifying the responses of SAW devices coated with zeolites embedded in a TEOS matrix. One method developed by Xu *et al.* takes advantage of synthesizing zeolites via the vapor phase.³⁰ Kim *et al.* have synthesized, using the vapor phase

method, uniformly thin films of ZSM-5 on a quartz surface treated with *ca.* 1 mm thick quiescent TPAOH solution, i.e., one drop of 40% TPAOH solution spread over a 1 cm² quartz surface.^{31,32} This pretreatment of quartz with TPAOH aids in the creation of active sites whereby the zeolite crystal can physically attach itself to the quartz substrate. After calcination, lithographically patterning a set of interdigitated electrodes onto this surface then creates a SAW device with a coating of pure ZSM-5. This eliminates the difficulty of accounting in a quantitative manner for the amount of adsorption attributable to the domains of embedding TEOS matrix. To further eliminate the effects of adsorption on the crystal surface, it is possible to chemically modify the surface silanol groups. For instance, treatment with triphenylchlorosilane may well minimize adsorption of water and other hydrophilic species on the surface by saturating the surface with aromatics. The agents used in such treatments must, however, be larger than the pore apertures so as to leave the interior porous network unaltered.

A second method also involves the synthesis of thin films directly onto the quartz substrate. Yan *et al.* reports the method of anchoring zeolite crystals through a molecular interface.³³ First, the surface of a quartz substrate is coated with a layer of gold by vapor deposition. Then monolayers of thiol-alkoxysilanes are attached to this gold surface to serve as the interfacial layer. The resulting monolayer-covered substrates were then transferred to a presonicated zeolite suspension for the subsequent adhesion of the zeolite crystals. Again, fabrication of electrodes on this surface produces the same sensor as that synthesized by the vapor phase method.

Although the development of new selective coatings will undoubtedly continue to improve SAW vapor sensor performances based on mass sensitivity,

new schemes to exploit the SAW sensitivity to coating conductance changes³⁴ or elastic modulus changes should afford new opportunities for imaginative chemical vapor sensor designs. Applications of other oscillation modes such as shear horizontal waves and flexural plate waves to sensing in the liquid phase are also subjects of active research. These types of sensors have found uses in measurements of immunochemical binding reactions³⁵ and liquid viscosities,³⁶ respectively.

As most reports show, the selectivity and sensitivity of a particular coating may be quite good for a specific analyte species under ideal conditions, i.e. inert environment without interfering gases, but for sensors to be practical, they must ultimately have the capacity to detect the presence of a great number and variety of gases. For this reason, an array of SAW sensors, much like a more complicated version of the simple two-device array proposed above, have received increasing attention.³⁷ In this approach, a limited number of sensors each coated with a different coating having preferential, but not unique, selectivity to a variety of vapors is exposed simultaneously to the vapor analyte. Each sensor responds to a differing degree depending on the type of vapor, and the resulting pattern of responses can then be used to identify certain preselected species, or classes of chemical vapors, in the ambient environment by applying a variety of pattern recognition algorithms.³⁸⁻⁴² Current advances in silicon micromachining has already produced miniature valves and other pneumatic hardware that can be used to support a futuristic SAW "chip." Presently, prototypes of SAW array sensors the size of a credit card have already been fabricated and tested.²¹ Thus, the success of integrating the traditionally engineering fields of systems and control into the

framework of fundamental chemistry should make chemical sensing with SAW devices a method of choice for chemical analysis in the future.

Conclusions

This study has demonstrated the importance of chemically selective coating layers in the sensing capabilities of SAW devices. Being qualitatively different materials, organic polymers and inorganic zeolites possess different physical properties that are at once an advantage and disadvantage with respect to the practical design of a chemical sensor. Devices coated with organic polymers have been shown to exhibit positive frequency shifts under various conditions. In particular, poly-(ethylenimine)-coated SAW oscillators show an increase in frequency upon exposure to humidified carbon dioxide (1-2% vol. CO₂), while poly-(4-vinylpyridine)-coated oscillators show similar changes in frequency at relative humidity levels below about 8%. Analysis of Auld's oscillation theory reveals the change in frequency is a function of the sum of two terms—a mass loading term and an elastic term. As the piezoelectric coefficients for the quartz substrate used in this study are negative, such response behavior suggests the importance of elastic effects in polymeric materials.

It is also shown that spin casting polymer solutions onto the device surface is more likely to generate uniformly thin films than spin coating suspensions of zeolite crystals. The latter has been found to yield well distributed domains of crystallites embedded on a supporting matrix. Larger crystals (micron-size) substantially scatter the acoustic wave energy, resulting in the complete dampening of SAW oscillations.

Sorption experiments reveal that all materials used have higher affinities for water vapor than for CO₂, with the frequency shifts for water generally being at least one order of magnitude larger than that for CO₂. In the case of poly-4-vinylpyridine (PVP) coatings, pulses of CO₂ produce no signals above the level of noise in the baseline. Additionally, when CO₂ and water are both present in the vapor stream, PVP-coated devices continue to show no detectable response to CO₂ while responding well to water vapor; thus, no interference is observed. This lack of interference is also found to be true for ZSM-5 coatings, as the SAW device continues to respond to pulses of CO₂ in the presence of water and vice versa. Signals from SAW devices with poly-ethylenimine (PEI) coatings, however, do exhibit significant hysteresis (in addition to the negative Δf frequency shifts described above) when both water and CO₂ are present. Although PEI-coated devices have high sensitivity and fast response times to humidified nitrogen alone, this interference phenomenon precludes the use of PEI as a viable coating material for the purpose of humidity sensing in real environments where CO₂ is likely to be present in significant quantities. However, an array of ZSM-5- and PVP-coated SAW devices can conceivably be designed to detect both humidity and CO₂ levels, as PVP coatings are sensitive only to water while ZSM-5 coatings are sensitive to both.

References

1. H. Wohltjen and R. E. Dessy, *Anal. Chem.* **1979**, *51*, 1458-1475.
2. H. Wohltjen, U.S. Patent No. 4,312,228.
3. H. Wohltjen, *Sens. Actuators* **1984**, *5*, 307-325.
4. D. S. Ballantine, Jr., and H. Wohltjen, *Anal. Chem.* **1989**, *61*, 704A-715A, and references therein.
5. A. d'Amico and E. Verona, *Sens. Actuators* **1989**, *17*, 55-66.
6. M. S. Nieuwenhuizen and A. Venema, *Sens. Mater.* **1989**, *5*, 261-300.
7. C. G. Fox and J. F. Alder, *Analyst* **1989**, *114*, 997-1004.
8. G. J. Bastiaans, in *Chemical Sensors*, T. E. Edmonds, Ed., Blackie: Glasgow and London, 1988, pp 295-319.
9. J. W. Grate and M. H. Abraham, *Sens. Actuators* **1991**, *3*, 85-111.
10. M. D. Ward and D. A. Buttry, *Science* **1990**, *249*, 1000-1007.
11. H. Bahadur and R. Parshad, in *Physical Acoustics*, W. P. Mason and R. N. Thurston, Eds., Academic Press: New York, 1982, pp 37-171.
12. V. E. Bottom, *Introduction to Quartz Crystal Unit Design*, Van Nostrand Reinhold: New York, 1982.
13. G. Sauerbrey, *Z. Phys.* **1959**, *155*, 206.
14. J. G. Brace, T. S. Sanfelippo, and S. G. Joshi, *Sens. Actuators* **1988**, *14*, 47.
15. S. J. Martin, A. J. Ricco, D. S. Ginley, and T. E. Zipperian, *IEEE Trans.* **1987**, *UFFC-34* (2), 143.
16. A. J. Ricco, G. C. Frye, and S. J. Martin, *Langmuir* **1989**, *5*, 273-276.
17. W. H. King, *Anal. Chem.* **1964**, *36*, 1735-1739.
18. R. M. White and F. W. Voltmer, *Appl. Phys. Lett.* **1965**, *7*, 314.
19. R. M. White, *Proc. IEEE* **1971**, *58* (8), 1238.
20. H. Wohltjen, Microsensors Systems Inc., 158MHz SAW Device Manual.
21. H. Wohltjen, D. S. Ballantine, Jr., and N. L. Jarvis in *Chemical Sensors and Microinstrumentation*; R. E. Dessy, W. R. Heineman, J. Janata, and W. R. Seitz, Editors,

- ACS Symposium Series 403, American Chemical Society: Washington, DC, 1989, pp 157-175.
22. B. A. Auld, *Acoustic Fields and Waves in Solids*, Wiley: New York, 1973, Vol. 2.
 23. J. W. Grate, A. Snow, D. S. Ballantine, H. Wohltjen, M H. Abraham, R. A. McGill, and P. Sasson, *Anal. Chem.* **1988**, *60*, 869-875.
 24. I. Langmuir, *J. Am. Chem. Soc.* **1918**, *40 (9)*, 1361.
 25. G. C. Grye and S. J. Martin, *Applied Spectroscopy Reviews* **1991**, *26 (1,2)*, 73-149.
 26. H. Fujita, in *Diffusion in Polymers*, J. Crank and G. S. Park, Eds., Academic: New York, 1968, Chap. 5.
 27. A. Zecchina, S. Bordiga, G. Spoto, L. Marchese, G. Petrini, G. Leofanti, and M. Padovan, *J. Phys. Chem.* **1992**, *96*, 4985-4990.
 28. T. Bein, K. Brown, G. C. Frye, and C. J. Brinker, *J. Am. Chem. Soc.* **1989**, *111*, 7640-7641.
 29. S. J. Gregg and K. S. W. Sing, *Adsorption, Surface Area and Porosity*, Academic Press: London, 1967.
 30. W. Xu, J. Dong, J. Li, J. Li, F. Wu, *J. Chem. Soc. Chem. Commun.* **1990**, 755-756.
 31. M.-H. Kim, H.-X. Li, and M. Davis, *Microporous Materials* **1993**, *1*, 191-200.
 32. M.-H. Kim, Ph.D. thesis, Blacksburg, VA, 1992.
 33. Y. Yan and T. Bein, *J. Phys. Chem.* **1992**, *96*, 9387-9393.
 34. J. J. Ricco, S. J. Martin, and T. E. Zipperian, *Sens. and Actuators* **1985**, *8*, 333.
 35. J. E. Roederer and G. J. Bastiaans, *J. Anal. Chem.* **1983**, *55*, 2333.
 36. A. J. Ricco and S. J. Martin, *J. Appl. Phys. Lett.* **1987**, *50 (21)*, 1474.
 37. D. S. Ballantine, Jr., S. A. Rose, J. W. Grate, and H. Wohltjen, *J. Anal. Chem.* **1986**, *58*, 3058-3066.
 38. W. P. Carey, K. R. Beebe, and B.R. Kowalski, *J. Anal. Chem.* **1987**, *59*, 1529-1534.
 39. W. P. Carey, K. R. Beebe, B. R. Kowalski, D. L. Illman, and T. Hirschfeld, *J. Anal. Chem.* **1986**, *58*, 149-153.
 40. S. L. Rose-Pehrsson, J. W. Grate, D. S. Ballantine, Jr., and P. C. Jurs, *J. Anal. Chem.* **1988**, *60*, 2801-2811.
 41. S. Zaromb and J. R. Stetter, *Sens. Actuators* **1984**, *6*, 225-243.
 42. F. L. Dickert and P. A. Bauer, *Adv. Mater.* **1991**, *3*, 436-438.